ASEG Extended Abstracts

ISSN: 2202-0586 (Print) (Online) Journal homepage: https://www.tandfonline.com/loi/texg19

Improving modelling of AEM data affected by IP, two case studies

Viezzoli Andrea, Vlad Kaminski, Yusen Ley Cooper, Lyndon Hardy & Gianluca Fiandaca

To cite this article: Viezzoli Andrea, Vlad Kaminski, Yusen Ley Cooper, Lyndon Hardy & Gianluca Fiandaca (2015) Improving modelling of AEM data affected by IP, two case studies, ASEG Extended Abstracts, 2015:1, 1-5, DOI: 10.1071/ASEG2015ab213

To link to this article: https://doi.org/10.1071/ASEG2015ab213

Published online: 22 Mar 2019.

ASEG-PESA 2015
Geophysics and Geology together for Discovery
24th International Geophysical Conference and Exhibition
15–18 February 2015 Perth, Western Australia

Improving modelling of AEM data affected by IP, two case studies

Viezzoli Andrea
Aarhus Geophysics Aps
C.F.Møllers Allè 4,
DK-8000 Aarhus C,DK
av@aarhusgeo.com

Vlad Kaminski
KM Geophysics
LLC, Vancouver
Canada
vlad@kmgeophysics.com

Yusen Ley Cooper
CSIRO
Kingston, WA
yusen.ley@csiro.com

Lyndon Hardy
Abra mining

Gianluca Fiandaca
Aarhus university
Denmark
gf@geo.au.dk

SUMMARY

Modelling IP parameters, including dispersive resistivity, from AEM data showing clear IP effects is possible. Using the spatially constrained inversion approach, with forward response that account for the full Cole and Cole model, we recover realistic chargeability and "IP corrected "resistivities sections from two VTEM datasets, from Canada and Australia. The "IP corrected" resistivity sections often show better agreement with known geological features, while improving dramatically the data fit, with respect to those obtained without IP modelling. While the majority of the IP effect originate from shallow chargeable layers, there seems to be some positive correlation between an isolated deep chargeable anomaly and known base metal deposit location.

Key words: Airborne EM, IP, VTEM, Chargeability, Cole-Cole, Mining, Spatially Constrained Inversion

INTRODUCTION

The occurrence of negative voltage values, or abnormal increased decay rates in central AEM systems is considered to be caused IP effects. In 1996, Smith and Klein treated a case of IP observed on GEOTEM data collected in the high arctic of Canada. but very rare studies were carried out, in the wake of this paper. The common approach has been to neglect negative values, or use them as indicators in the decay where noise levels are lower than to those of signal. Kratzer and Macnae (2012) processed VTEM data acquired in Africa providing a chargeability distribution. Other preliminary results were provided by Viezzoli et al. (2013). In this paper we show two different case-studies: Mt. Milligan in British Columbia (Canada) and Abra in the Capricorn Orogen in WA.

METHOD AND RESULTS

The data were fist processed to reduce noise, then inverted with AarhusInv inversion code (previously known as em1dinv), modified as per Fiandaca et al. (2012). It is able to solve for Complex Impedance, using the model of Cole-Cole (1941), providing combined estimation of ρ, c, m and τ Care must be exerted with data preparation, regularization and choice of starting models. For example, c and τ are bound to be very poorly determined, and so need to be treated with caution and can be fixed to nominal values. We also performed 3D inversion of magnetic VTEM data in one of the 2 case studies to constrain the interpretation.

CASE 1: MT. MILLIGAN

Mt. Milligan is a large Cu-Au porphyry deposit located in central British Columbia. Multiple geophysical data sets were collected over Mt. Milligan, including airborne VTEM survey (EM and magnetic) in 2008. The EM data were inverted using Cole-Cole model in order to extract IP information, including chargeability of the subsurface using SCI concept (Viezzoli et al, 2013). Further, the Magnetica data TMI data were inverted using UBC-GIF approach (Li and Oldenburg, 1996). From geological evidence the Mt. Milligan deposit is a mineral occurrence within a porphyrite-monzanite stock (MBX), hosted within andesites and volcanites of the Takla group (DeLong et al, 1991). Monzonite intrusives are often accompanied by intense hydrothermal alteration processes. In the case of the Mt. Milligan deposit there are two types of alteration present: potassic and propylitic. Potassic alteration produces chalcopyrite, bornite and magnetite, while propyllitic alteration produces pyrite and minor magnetite. These alterations affect different physical properties of the strata which is reflected in the inversion models. The 3D magnetic inversion can be useful in recovering information about the magnetite contents and therefore can be indicative of areas subjects to potassic alteration, while the chargeability of the rocks may be affected by presence of pyrite, chalcopyrite and bornite. Chargeability is a particularly important physical property sensitive to presence of gold in porphyry deposits, where faint magnetic or conductive EM anomalies may be detectable. Figure 1 demonstrates the correlation between the map of alterations at Mt. Milligan and the planar distribution of magnetic susceptibility at the depth of 50 m below surface. In Figure 2 a similar correlation is shown in a cross-section. The EM data, retaining all the IP, was then inverted with SCI using the Cole-Cole model. The results of the inversions of Cole-Cole parameters are realistic, with peaks of chargeability m0 corresponding to the location of the negative or very fast decaying transients. We further compare the inverted chargeability sections with available geological and geophysical ancillary information. Oldenburg et al., (1997) presented results of inversion of chargeability from ground IP data from this area. The central part of line 540 of the VTEM survey (Figure 1) corresponds to a ground IP profile. Figure 3 presents the comparison between the airborne derived chargeability section and the chargeability recovered by Oldenburg from ground IP data. The comparison shows a positive correlation between the near surface chargeability recovered from the ground IP and the VTEM airborne derived chargeability section. The deeper chargeable anomalies from the ground survey associated with MBX stock are not recovered from this VTEM dataset.

Oldenburg et al. showed that the chargeability maxima, including the shallower ones, are often correlated with gold mineralization. AEM derived shallow chargeability is mainly located on the western border of WBX and on DWBX.

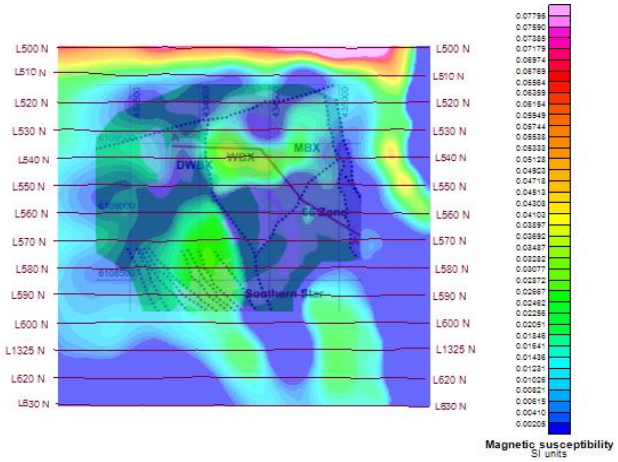

Figure 1. Results of the 3D magnetic inversion of VTEM data flown over Mt. Milligan deposit.

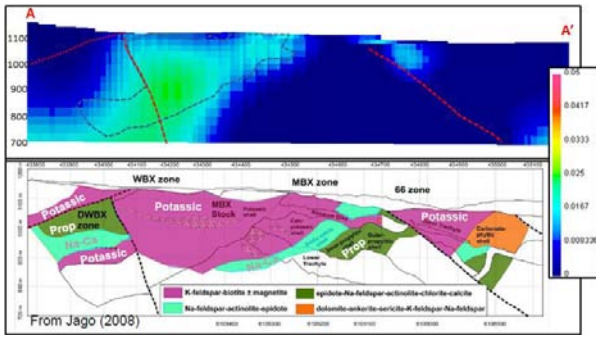

Figure 2. The recovered magnetic susceptibility from a 3D inversion matched with the AA' cros-section (in Figure 1).

The shallow chargeability is concentrated to the W, SW of the WBX stock. This seems to confirm the discussion by Oldenburg et al. where it was suggested that the strongest IP response might be manifested as a halo found outboard of the primary mineralization, associated to increase of pyrite concentration as one enters regions of propylitic alteration.

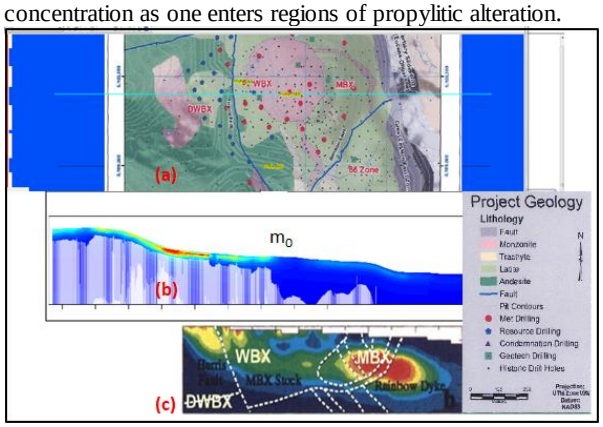

Figure 3. Comparison between (a): Mt. Milligan Geology; (b): Airborne recovered m0 parameter (VTEM data); (c): Ground recovered chargeability (Oldenburg et al, 1997).

CASE 2: ABRA

The Abra deposit is a base metal located in the eastern part of the Capricorn orogen, a geological province where there is recorded evidence of a complex history of deformation, metamorphism and magmatism. The mineralisation at Abra was found by targeting a confined regional magnetic high show as a profile (magenta) in Figure 4, and has been intersected at depth of around 300m by several drill holes .As in the Mt Milligan case, the VTEM data were inverted both 1) without modelling IP parameters (treating all negatives as noise) and 2) modelling IP parameters (retaining all negatives). Figure 4 shows a comparison (Line 4040) between CSIRO's 30 layers inversion using the GA-LEI (Brodie 2012) without IP modelling, and Aarhus Inv's 25 layers inversion accounting for and modelling the IP. Geology and satellite imagery used in Figure 4) as reference.

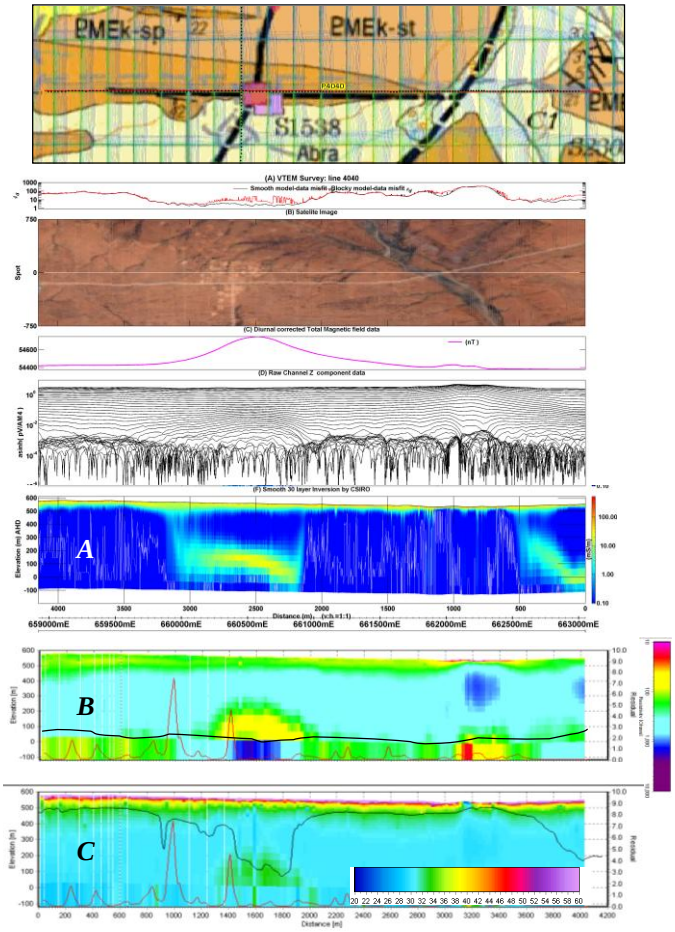

Figure 4. Line 4040. From top, geology, satellite imagery, data plot, GA LEI (section A), resistivity recovered accounting for the IP effect (B, depth of investigation in black, misfit in red), chargeability (C).

All sections (resistivity without IP, resistivity with IP, chargeability) do show an anomaly in the proximity to the known lateral location of the mineral deposit. Section A, however, shows both poor data fit and resistivity values anomalously high for the host rock (sandstones). This is the result of trying to fit an anomalously fast, IP-affected, EM transient. The resistivity section obtained modelling IP (B) fits the data significantly better and produce more realistic resistivities for the host rock. It also shows better match with geology (outcrop and faulting). The chargeability section shows very near surface highly chargeable layers (possibly iron

rich cover) across most of the section . It also recovers an indication of a chargeable anomaly at depth, in the proximity to the know mineralization. Admittedly this anomaly is very proximal to the estimated depth of investigation, hence could be easily questioned. On the other hand it shows similarities with ground IP anomalies gathered in the proximity of this flight line. At this stage no conclusive remark cane be drawn regarding this deep chargeable anomaly, future developments will soon be presented. Even though a rare occurrence, it can be shown that certain combinations of chargeability and resistivity can produce measurable IP effects on VTEM data. Figure 5 displays results from where a coincident airborne and ground IP/resistivity line has been acquired. Once again, the resistivity section obtained modelling airborne IP produces results that fit the measured data, and are consistent with the available geological information. Notice the good correlation with outcrop geology, especially considering that the first gate of the system was at approximately 80 µs after end of ramp, and therefore the near surface resolution is expected to be limited. As shown in the figure the coincident line of airborne derived resistivity (accounting for IP) also matches better the resistivity section obtained from ground resistivity survey. In Figure 6 a geological cross section (with drillings) over the mineralization is overlain with the different inversion results from another line of VTEM data flown directly over the deposit.

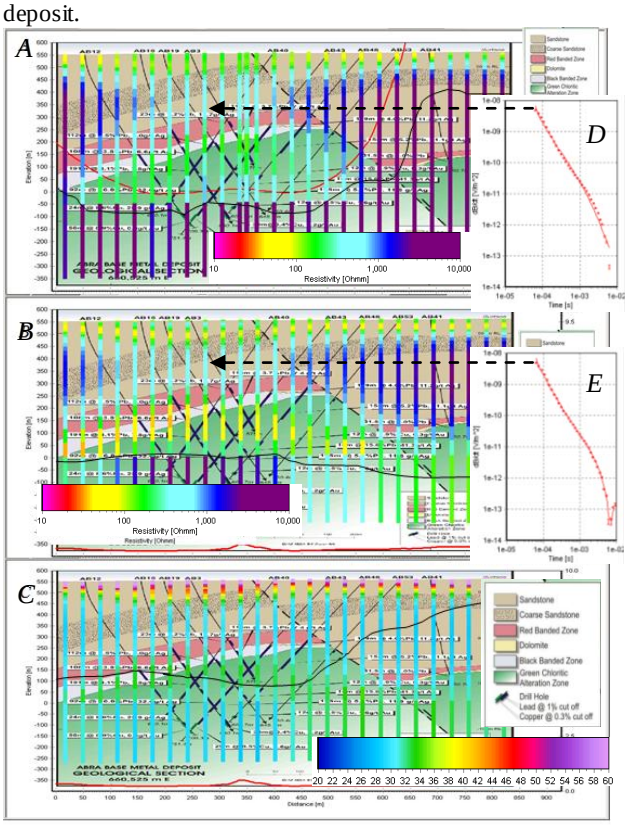

Figure 6. Comparison of airborne EM inversions with and without IP modelling versus geological section and drillings. (*A*) resistivity section obtained from VTEM data deleting all negatives, but not modelling IP parameters; (*B*) resistivity section obtained from VTEM data retaining all negatives, and modelling IP parameters; (*C*) Chargeability section obtained from VTEM data retaining all negatives; (*D*) measured data (errorbars) and forward response (continuous line) for a given model, without modelling IP parameters; (*E*) measured data (errorbars) and forward response (continuous line) for a given model, modelling IP.

The resistivity obtained without IP modelling shows a resistivity low centred approximately around the known mineralization. A sounding from this area displays poor data fit and suspect high values for the sandstones. The resistivity obtained with IP modelling seems to follow alteration zones or some sort of lithological boundary while fitting the data significantly better, producing more realistic values for the sandstones, and recovering better the known geology, including faults. The chargeability section seems to have some correlation with the known mineralization and ground IP models but the same caution suggested for line 4040 should be exerted also here.

CONCLUSIONS

Modelling trough inversion IP parameters in IP affected AEM data can produce improved resistivity, and realistic chargeability models. The case studies show that the resistivity obtained match ancillary information better than that obtained without taking IP into account. The chargeability sections also seem credible in the near surface. More work is needed to confirm to what extent the positive correlation between a deep chargeable anomaly and know mineralization is data driven.

REFERENCES

Brodie, R. C., (2012), Appendix 3: GA-LEI Inversion of TEMPEST Data, in The Frome airborne electromagnetic survey, South Australia: implications for energy, minerals and regional geology
edited by I. C. Roach, pp. 278-287, Geoscience Australia Record 2012/40-DMITRE Report Book 2012/00003

Cole, K. S., and Cole, R. H., 1941, Dispersion and absorption in dielectrics: Journal of Chemical Physics, 9-4, 341–351.

Espinosa and Labrenz, 2008, Geophysical assessment of the Mt Milligan Claims, Report prepared for Terrane metal Corps.

Fiandaca, G., Ramm, J., Binley, A., Gazoty, A., Christiansen, A. V., and Auken, E., 2012, Resolving spectral information from time domain induced polarization data through 2-D inversion: Geophysical Journal International.

Kratzer, T., and Macnae, J.C., 2012, Induced polarization in airborne EM: Geophysics, 77, E317-E327.

Li,Y.,Oldenburg,D.,1996, 3D Inversion of Magnetic Data, Geophysics (61-2), 394-408.

Oldenburg, D.W., Li, Y., Ellis, R.G., 1997, Inversion of geophysical data over a copper gold porphyry deposit: A case history for Mt. Milligan, Geophysics, 62-5, 1419-1431.

Smith, R.S., and Klein, J., 1999, A special circumstance of airborne induced polarization measurements: Geophysics, 61, 6-73.

Viezzoli, A., Christiansen, A.V., Auken, E., and Sorensen, K., 2008. Quasi-3D modelling of airborne TEM data by spatially constrained inversion: Geophysics, 73, F105-F113.

Viezzoli A., Fiandaca, G., Segio, S., Auken., E., 2013, Constrained inversion of IP parameters from Airborne EM data, ASEG-PESA Expanded abstracts, Melbourne, Australia.

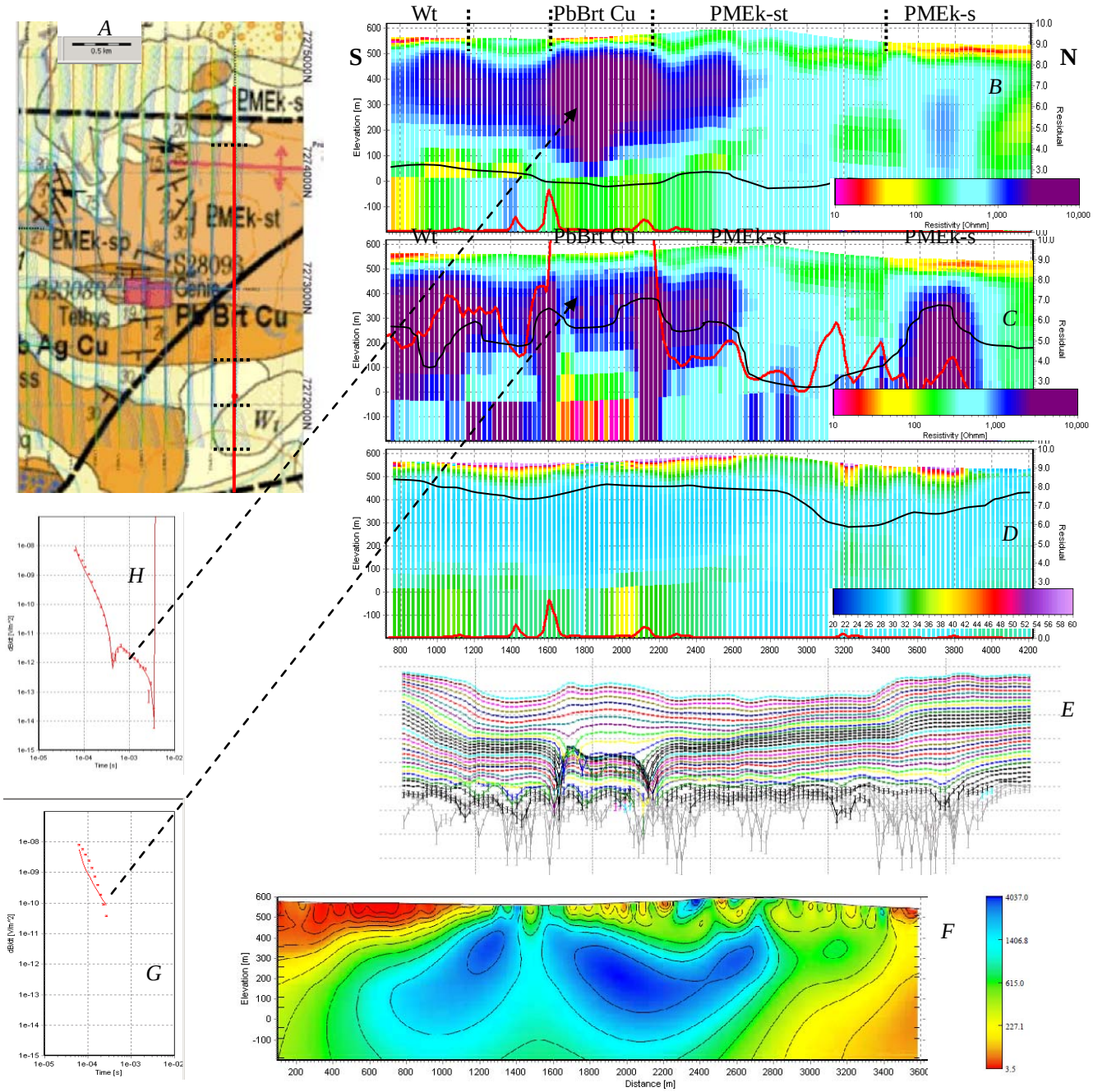

Figure 5. Comparison of inversions with and without IP modelling versus surface geology and ground geophysics. From top left, clockwise. (*A*) Geology of the area few km to the east of Abra deposit (WA); (*B*) resistivity section obtained from VTEM data retaining all negatives, and modelling IP parameters; (*C*) resistivity section obtained from VTEM data deleting all negatives, and not modelling IP parameters; (*D*) Chargeability section obtained from VTEM data retaining all negatives, and modelling IP parameters; (*E*) Measured VTEM data for these sections; (*F*) resistivity section obtained from ground geophysics (IP survey) over portion of the VTEM line (notice different colorscale); (*G*) measured data (errorbars) and forward response (continuous line) for a given model, without modelling IP parameters; (*H*) measured data (errorbars) and forward response (continuous line) for a given model, modelling IP parameters.